JOURNAL OF MATERIALS SCIENCE 37 (2002) 4013–4017

Fibrillation of aramid fiber using a vibrating ball mill and evaluation of the degree of fibrillation

A. HASHIMOTO*, M. SATOH, T. IWASAKI, M. MORITA
Department of Chemical Engineering, College of Engineering, Osaka Prefecture University, 1-1 Gakuen-cho, Sakai, Osaka 599-8531, Japan
E-mail: a-ha@pop21.odn.ne.jp

Methods of fibrillation of aramid fiber for a fiber-dispersion type of composite and evaluation of the degree of fibrillation were investigated. Continuous fibrillation of aramid fiber was carried out using a vibrating ball mill. The morphology of the fiber surface was controlled by adjusting the processing time of the fiber in the mill. An index based on image analysis was proposed to represent the morphological changes of treated fiber. The interaction between powder bed and fiber was determined by measuring the force required to pull a single fiber out of a compacted powder bed. The interaction between powder and fiber increased with the degree of fibrillation.

1. Introduction

Aramid is a strong, heat and wear resistant fiber that can be used in functional composite materials in combination with various materials. Highly fibrillated aramid fiber (pulp) has replaced asbestos fiber as one the key additives in the friction brake-pads of vehicles [1].

Commercially available aramid fiber is usually a single straight filament with a round cross-section and a very smooth surface. When used as a brake-pad additive, the chopped and fibrillated fiber is mixed with various powdered materials such as inorganic and organic compounds, metals and phenolic resin binders. Dispersing the fibrillated fiber, i.e., the minute fibrils, in the powder bed effectively forms a fiber-fiber network, holding the powdered materials, increasing the strength of the compaction and improving the wear of the brake-pad.

On the other hand, the tensile strength of the fibrillated fiber is lower than that of non-fibrillated fiber due to thinning of the trunk fiber [2]. Therefore, it is necessary to control the fibrillation to a suitable degree for the fiber-dispersion type of composite. To control the morphology and/or degree of fibrillation of the fiber, many methods including mechanical and physicochemical treatment have been proposed and employed. For instance, fibers have been extruded through specially shaped orifices, sheared and ground with a mill, and treated with an air jet [3, 4], laser beam or plasma [5]. The morphology of the fiber has been evaluated by SEM observation, specific surface area [6] or mechanical properties. Few studies evaluating the degree of fibrillation have been reported.

In this study, continuous fibrillation tests were carried out using a vibrating ball mill to control quantitatively the state of the fiber surface. A conventional index based on analyzing the appearance of the treated fiber is proposed to represent the degree of fibrillation. Furthermore to evaluate the interaction between powder bed and fiber, a single-fiber pull-out test was performed, and the correlation between the tensile force necessary to remove a fiber from the powder bed and the degree of fibrillation is discussed.

2. Material and experimental apparatus

2.1. Aramid fiber

The aramid fiber used in this study (Kevlar 29: DuPont/Toray Co., Ltd) was supplied as multifilament yarns. A single filament had the following representative physical properties: an average diameter of 17 μm, a true density of 1440 kg/m^3, a round-shaped cross-section, a tensile strength of 2.9 GPa, and a thermal decomposition point of 810 K. Fig. 1 shows a SEM photograph of a single untreated fiber and its chemical structure. The single fiber consists of very fine filaments, called "fibrils," with a mean diameter of 0.6 μm [7].

2.2. Continuous fibrillation system

Fig. 2 is a schematic diagram of the continuous fibrillation system. The main part of this system is a cylindrical vessel (inner diameter 135 mm and length 250 mm) set horizontally on a vibrating bed (sinusoidal wave at 60 Hz). Two different sizes of stainless steel balls (9.53 mm and 4.76 mm in diameter) were added to aid fibrillation, in a weight ratio of 3 : 2. A loop of the fiber sample (multifilament) was continuously passed through the ball section at a constant rate (2.4 mm/s). The tension of the fiber was regulated at a constant value of 3 N by a tension pulley and spring during the operation. The total amount of the energy applied to the fiber sample was controlled by changing the operating

*Author to whom all correspondence should be addressed.

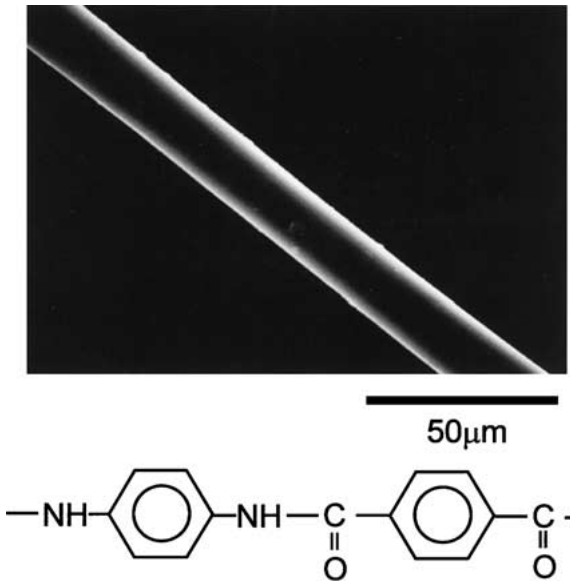

Figure 1 SEM photograph of an aramid fiber and the chemical structure.

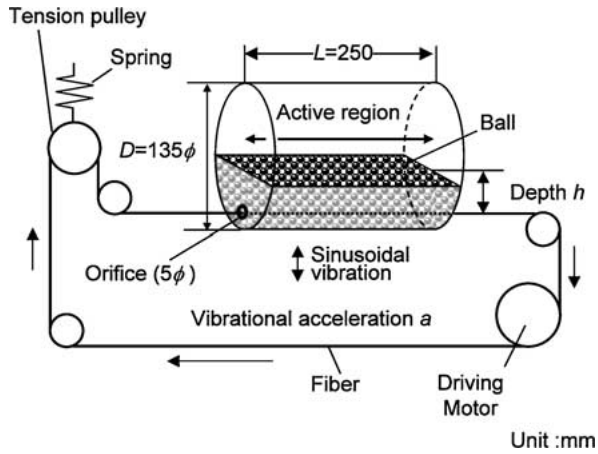

Figure 2 Schematic diagram of the continuous fibrillation system.

conditions as follows: a (m/s^2) = vibrational acceleration, h (m) = the depth of the path of the fiber through the ball layer, and t (min) = the net processing time in the ball layer (treatment time).

3. Results and discussion

3.1. Fibrillation and evaluation of the degree of fibrillation

The appearance of a fiber after passing through the fibrillation system is compared with the original fiber is Fig. 3. It is clear that the fibrillation increases with treatment time, t (see, (b) through (d)) due to the compressive and shearing force of the balls in the vibrating mill. The diameter of each fibril after the treatment was around 0.5–1.0 μm, which corresponds with the approximately 0.6 μm reported in a study by Panar *et al*. [7]. In the case of over-treatment (after 400 min), the fine fibrils were disintegrated and had fallen off the trunk fiber, as seen in Fig. 3e.

To evaluate the effect of the treatment on the fiber, the tensile strength of a single fiber was tested with a gauge length of 40 mm and a tensile speed of 0.035 mm/s. Fig. 4 shows the decrease of tensile strength, $F_{\max}$, at the fracture point, with increasing treatment time, t. The tendency of $F_{\max}$ to decrease does not represent the actual degree of fibrillation but only the thinning down of the trunk of the fiber. Therefore, to evaluate the degree of fibrillation directly, image analysis was carried out. Fig. 5 illustrates the procedure of sample preparation for image analysis. A single treated fiber was fixed on the slide glass, and air was blown from one side to spread and orient the fibrils at a right angle to the direction of the trunk. The projecting area of the fiber was measured by a CCD camera attached to an optical microscope (BH2-UMA: Olympus) and image analyzer (Luzex FS: Nireco). The minimum size resolution of image was set at 2.65 μm/pixel, and the size of the window was set at 1330×1270 μm. By scanning the viewing window along the fiber trunk, the projecting area, S_i (μm^2), of the fibrils in the range of 1000 μm of fiber was measured. The average value of the projected areas, S is calculated by

$$S = \frac{1}{n}\sum_{i=1}^{n} S_i \tag{1}$$

where n is the sample number (in this study, $n = 50$)

Fig. 6 shows the relationship between S and treatment time t compared with the tensile strength, $F_{\max}$. The value of S reached its maximum at $t = 200$ min, while $F_{\max} - t$ curve showed a tendency to steadily decrease in the whole experimental range. Over-treatment cuts and tears fibrils from the trunk. The time range for controlling the fibrillation is within 200 minutes of treatment using the vibrating ball mill operating under the above-mentioned conditions.

From the point of view of practical application, the degree of fibrillation, ψ, is defined based on the data of image analysis in the range of $0 \leqq t \leqq 200$ (min).

$$\psi = \frac{S - S_0}{S_{\max} - S_0} \tag{2}$$

where, S_0 is the projected area of untreated fiber of 17000 μm^2 (diameter 17 $\times$ length 1000 μm), and $S_{\max}$ is the extrapolated value for the empirical equation that approximates the experimental data of S as a function of the exponential equation.

The ideal value of the $S_{\max}$, based on 800 fibrils in a single fiber trunk and a sample length of 1000 μm, should be 4.8×10^5 μm^2. However, this $S_{\max}$ value is not realistic because not all fibrils form a monolayer plane without overlap. In a sense, the degree of fibrillation proposed here is a conventional definition.

Fig. 7 shows the relationship between the relative tensile strength, $\bar{F}$, defined as the ratio of tensile strength between treated fibers and untreated fibers and the degree of fibrillation, ψ. It is clear that the new index, ψ, defined here shows a comparable diminution of the relative tensile strength, $\bar{F}$. The value of F at $\psi = 1$ was calculated at about 20% of the value for the untreated fiber. Thus, the utility of image analysis for the evaluation of fibrillation is confirmed within the above-mentioned observation range, $S_0 < S < S_{\max}$.

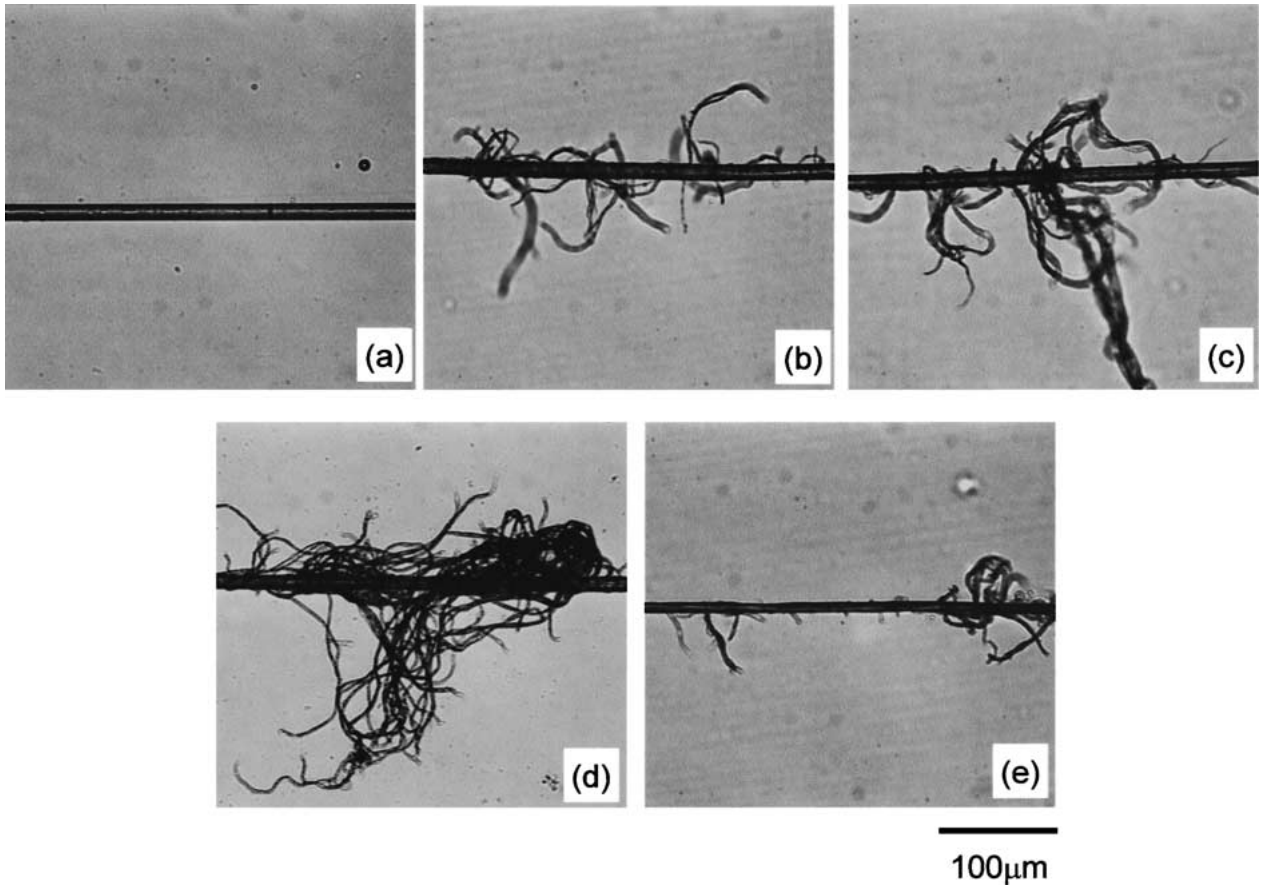

Figure 3 The appearance of a fiber after passing through the fibrillation system: (a) original (b) 50 min (c) 120 min (d) 200 min (e) 400 min.

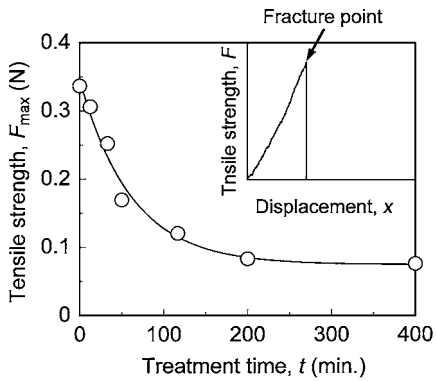

Figure 4 Relationship between tensile strength, F_{max} at the fracture point and the treatment time, t.

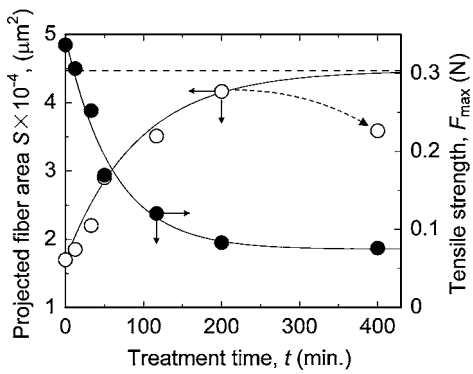

Figure 6 Relationship between the projected fiber area, S and treatment time, t compared with the tensile strength, F_{max}.

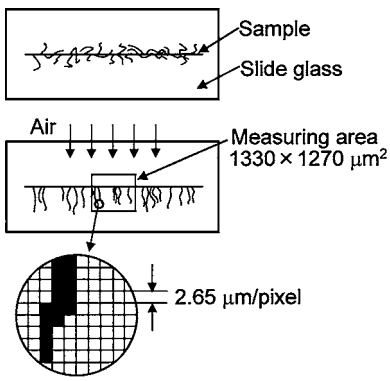

Figure 5 The procedure of sample preparation for the image analysis.

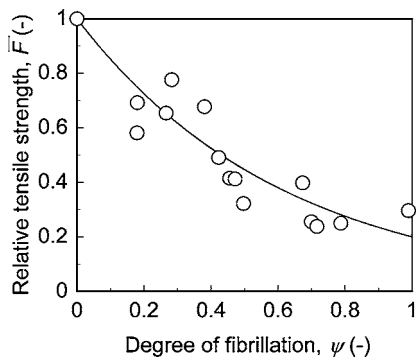

Figure 7 Relationship between the relative tensile strength, $\bar{F}$ and the degree of the fibrillation, ψ.

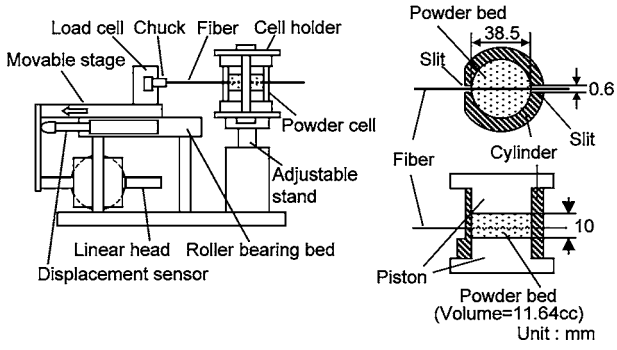

Figure 8 Schematic diagram of a constant-volume powder tester.

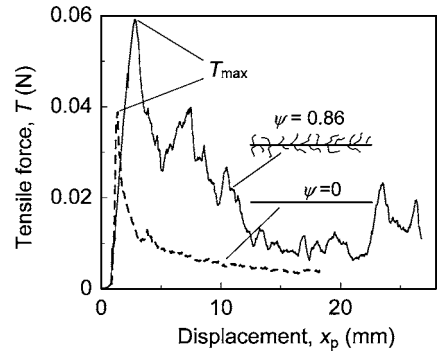

Figure 9 Typical tensile force, T versus displacement, x_p curves comparing treated fiber with non-treated fiber, pulling rate; 0.35 mm/s, void fraction of powder bed; $\varepsilon = 0.64$.

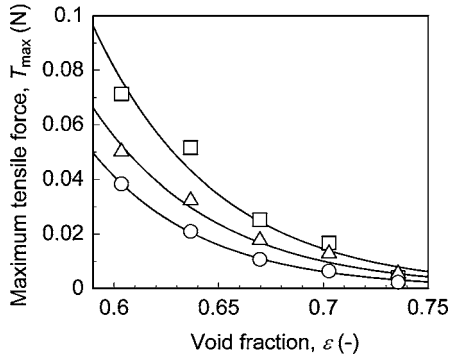

Figure 10 Relationship between the maximum tensile foce, T_{max} and the void fraction of powder bed, ε (○) $\psi = 0$; (△) $\psi = 0.468$; (□) $\psi = 0.862$.

3.2. Fiber/powder interaction

To investigate the effects of surface treatment of the fiber on the compounded state from the viewpoint of interaction between the fiber and the matrix material, a new device, which consists of a powder cell and a load cell to measure the force required to pull a single fiber out of the compacted powder bed, was designed. A schematic diagram of a constant-volume powder tester is shown in Fig. 8. The powder cell placed on the adjustable-height stand was a simple acrylic resin piston-cylinder type vessel (inner diameter: 38.5 mm, height: 10 mm, effective volume: 11.64 cc). There were two parallel slits 0.6 mm wide in the sides of the cylinder wall to pull the fiber through the powder bed horizontally with minimal contact friction with the cylinder wall. A strain-gauge load cell was set on the movable stage supported on a horizontal roller bearing bed with a displacement sensor. One end of the fiber was clamped by a chuck attached to the tip of the load cell and pulled at the desired rate by the motor with a linear head. In this study, calcium carbonate powder (Maruo Calcium Co. Ltd.; mean size: 2.7 μm, true density: 2600 kg/m^3) was used as the sample to test the tensile force of the pull-out. Tensile force, T versus displacement, x_p was measured by the following procedure. (1) A certain quantity of the sample powder to be packed (void fraction) in the cell was accurately measured. (2) Half of the sample powder was packed into the cell and pressed to flatten the powder surface. (3) The fiber was stretched out straight on the surface of the powder bed. (4) The cell was set on the stand, and one end of the fiber was connected to the load cell to start a test run.

Fig. 9 shows the typical tensile force, T, versus displacement, x_p, curves comparing treated fiber with non-treated fiber measured under the same conditions (pulling rate: 0.35 mm/s and void fraction of powder bed: $\varepsilon = 0.64$). In the figure, dashed and solid lines indicate the curve for the untreated and the treated fibers, respectively. Both data sets showed a maximum peak at the initial stage of the displacement and then decayed toward steady values.

In the case of untreated fiber ($\psi = 0$: smooth surface), T_{max} was smaller than that of the treated fiber, and the shape of the decay curve showed a steady, smooth line. On the other hand, in the case of treated fiber ($\psi = 0.86$), T_{max} increased and the decay curve fluctuated irregularly. The variations of these characteristic curves might include various kinds of interactive factors among the conditions of the fiber surface and the powder properties. T_{max} was considered as the representative value for the transitional point from static to dynamic behavior of pulling out.

Fig. 10 shows the relationship between the maximum tensile force, T_{max}, and the void fraction of the powder bed, ε as a parameter of ψ. T_{max} increased as the void fraction decreased, not only because of increases in contact points between fiber and powder, but also among the matrix powder particles. In a sense, it is obvious that more-fibrillated fiber can be held more strongly by matrix powders. Thus, T_{max} increased with ψ as seen in the figure.

4. Conclusions

A mechanical system for treating the surface of the filler fiber was developed, and its performance was evaluated. The morphology of treated fibers and the interaction between powder and fiber were studied. The results can be summarized as follows.

1. Use the vibrating ball mill was effective for continuous fibrillation of aramid fibers, and the morphology of the treated fiber surface can be controlled by adjusting the operating conditions, for example, the processing time of fiber in the mill.

2. Within the operating condition for peeling away of fibrils from the fiber trunk, the degree of fibrillation, ψ, defined here based on the image analysis was a useful index to express the morphological changes of the fiber surface with treatment time.

3. A larger ψ indicated higher resistance to being pulled out of the powder bed, i.e., availability of fibrillation for the compounding of fiber/powder system was demonstrated by using a simple, newly designed single-fiber pull-out tester.

References

1. D. G. SWARTZFAGER, R. SENIGO and EUAN PARKER, SAE paper 982255, 1998.
2. S. J. DETERESA, S. R. ALLEN, R. J. FARRIS and R. S. PORTER, *J. Mater. Sci.* **19** (1984) 57.
3. A. DEMIR, M. ACAR and G. R. WRAY, *Textile Res. J.* **58** (1988) 318.
4. J. SRINIVASAN, A. K. SENGUPTA and V. K. KOTHARI, *ibid.* **62** (1992) 40.
5. M. R. WERTHEIMER and H. P. SCHREIBER, *J. Appl. Polym. Sci.* **26** (1981) 2087.
6. S. F. WASEEM, S. D. GARDNER, G. HE, W. JIANG and U. PITTMAN, *J. Mater. Sci.* **33** (1998) 3151.
7. M. PARNAR *et al.*, *J. Polym. Sci.* **21** (1983) 1955.

Received 25 October 2000
and accepted 29 March 2002